Extreme Mechanics Letters 80 (2025) 102399

Contents lists available at ScienceDirect

Extreme Mechanics Letters

journal homepage: www.elsevier.com/locate/eml

Ratcheting induced crack growth in semiconductor devices

Chenghai Li [a], Shao-Chen Tseng [b], Yu Zhou [a], Chieh-Hao Hsu [b], Wei-Hsiang Tu [b], Kuo-Chin Chang [b], Jun He [b], Zhigang Suo [a,*]

[a] John A. Paulson School of Engineering and Applied Sciences, Harvard University, MA 02138, United States
[b] Taiwan Semiconductor Manufacturing Company, Ltd., Hsinchu, Taiwan

ARTICLE INFO

Keywords:
Ratcheting
Semiconductor devices
Plasticity
Crack growth

ABSTRACT

Semiconductor devices integrate dissimilar materials, including semiconductors, ceramics, metals, and polymers. These materials have different coefficients of thermal expansion, so that the devices develop stresses when temperature changes. Here we study a failure mode caused by cyclic changes in temperature. Under certain conditions, thermal cycling causes a metal to accumulate plastic deformation cycle by cycle, a phenomenon called ratcheting. The ratcheting in the metal can drive a crack to grow in a nearby brittle material. We simulate a representative structure using the finite element method. As the temperature cycles, the plastic deformation in the metal ratchets, and the energy release rate of the crack in the brittle material increases. After a large number of temperature cycles, the metal no longer ratchets, and the energy release rate plateaus. We find that this plateau is well approximated by the energy release rate in a structure where the metal is replaced by a void, calculated by a monotonic change in temperature. This simplification reduces computational cost for modeling ratcheting induced cracking. We also examine the effects of material and geometric parameters. It is hoped that this study will aid the design of semiconductor devices.

1. Introduction

A semiconductor device integrates dissimilar materials in complex geometries [1–3]. Consider a specific example (Fig. 1a). During fabrication, a silicon die is first attached to an organic substrate through solder reflow at an elevated temperature typically around 220 °C [4]. After cooling to room temperature, a polymer underfill is dispensed and cured at $T_0 = 150$ °C to reinforce the solder joints and improve reliability [4]. As a common industrial practice to assess reliability, the structure is cycled between two temperatures [5], e.g., −40 °C and 125 °C, up to 1000 cycles (Fig. 1b). The dissimilar materials have different coefficients of thermal expansion. As temperature changes, the structure develops a stress field, which concentrates near the die corners.

Near a die corner, a copper line is surrounded by an etch stop layer (ESL) and an extreme low-κ dielectric (ELK) (Fig. 1c). The copper line serves as an interconnect due to its high electrical conductivity [6,7]. Under thermal cycling, the copper line can undergo plastic deformation [8]. ESL functions as a barrier or structural layer, and is brittle [3,6]. ELK insulates the copper line and reduces parasitic capacitance [2]. To reduce permittivity, highly porous ELK is used, which makes it extremely brittle, prone to debonding and cracking [2,9]. For example, debonding is often observed at both ESL-ELK and Cu-ELK interfaces after thermal cycling (Fig. 1c). Understanding these failure modes is essential for interpreting reliability tests and guiding device designs. This paper describes a mechanism by which thermal cycling drives a crack to grow cycle by cycle.

2. A qualitative understanding of ratcheting induced crack growth

The integrated structure in a semiconductor device is complex. To illustrate the basic mechanics, we study debonding between two brittle materials, ESL and ELK, caused by ratcheting plastic deformation in copper using a simplified structure (Fig. 2a). The substrate has a larger coefficient of thermal expansion than the silicon die (Fig. 1a). The underfill is cured at 150 °C. Upon cooling, the mismatch in the coefficients of thermal expansion of the substrate and the silicon die causes a shear stress at the die-substrate interface, pointing toward the center of the die. The reliability of the structure is assessed by a thermal cycling test (Fig. 1b). During the test, the temperature changes, but stays below the curing temperature of the underfill. Consequently, the shear stress at

* Corresponding author.
E-mail address: suo@seas.harvard.edu (Z. Suo).

https://doi.org/10.1016/j.eml.2025.102399

Available online 31 August 2025
2352-4316/© 2025 Elsevier Ltd. All rights reserved, including those for text and data mining, AI training, and similar technologies.

the die-substrate interface does not change direction and always points toward the center of the die. This unidirectional shear stress is further transferred through the underfill to ELK and copper. At the die-substrate interface, the shear stress varies with the position and temperature. To simplify the discussion, we will assume a constant shear stress, τ_0.

The thermal expansion mismatch also causes other stress components in copper. To illustrate the idea, consider a simplified stress state in which the copper is under unidirectional shear stress of a constant magnitude, τ_0. Furthermore, the mismatch in the coefficients of thermal expansion between copper and the surrounding materials also causes a cyclic normal stress in the horizontal direction, σ. The copper is taken to be a non-hardening material. For simplicity, we further assume that the yield strength of copper, σ_Y, is constant, independent of temperature. Under the combined stresses, τ_0 and σ, the metal yields when the magnitudes of the two stresses fall on an ellipse: $\sigma^2 + 3\tau_0^2 = \sigma_Y^2$ (Fig. 2b).

When the combined stresses satisfy the yield condition, the copper deforms plastically. As the temperature cycles, the increment of normal plastic strain, $d\varepsilon^P$, in the horizontal direction also cycles, but the increment of shear plastic strain, $d\gamma^P$, accumulates cycle by cycle, always in the same direction. This unidirectional accumulation of plastic strain is called ratcheting.

The ratcheting phenomenon in semiconductor devices and thin film structures has been studied before [10–14]. For a silicon die attached to a substrate, cracking was observed in a silicon nitride (SiN) film over aluminum pads near the die corner [12]. Caused by ratcheting plastic deformation, the stress relaxes in the aluminum but builds up in the SiN film, leading to fracture. Another related study analyzed the crawling of a blanket metal film on a silicon substrate [10]. When temperature cycles, the metal film accumulates plastic shear deformation directed by the unidirectional shear stress. Both studies focus on the evolution of plastic deformation and stress redistribution.

In the current work, we extend the analysis by calculating the energy release rate of a crack. For the structure in Fig. 2a, as temperature cycles, the plastic deformation in the copper ratchets. Consequently, the energy release rate of a crack at the ESL-ELK interface increases. After many thermal cycles, the copper no longer ratchets, behaves like a void, and the energy release rate plateaus. The buildup of the energy release rate causes a crack to grow in the nearby ESL-ELK interface.

3. Ratcheting plastic deformation redistributes stress

We first simulate the structure in Fig. 2a without a crack in Abaqus to ascertain the mechanism of ratcheting plastic deformation. Geometric parameters are listed in Table 1. The width w and the thickness t refer to the horizontal and vertical dimensions, respectively. The aspect ratio of copper is defined by w_{Cu}/t_{Cu}.

ESL and ELK are modeled as linear elastic materials. For ESL, we use a Young's modulus $E = 295$ GPa [15], Poisson's ratio $\nu = 0.24$ [16], coefficient of thermal expansion $\alpha = 3.8$ ppm/°C [17]. For ELK, we use $E = 10.5$ GPa, $\nu = 0.22$, $\alpha = 6.8$ ppm/°C [18]. For simplicity, copper is modeled as an elastic-perfectly plastic material. We use $E = 130$ GPa, $\nu = 0.34$, $\alpha = 16.5$ ppm/°C [18]. The yield strength of copper σ_Y varies from 100 to 170 MPa [19]. The structure is assumed under plane strain conditions. The top boundary is fixed in both directions ($u_x = u_y = 0$). The left and right boundaries are traction-free. A constant shear stress τ_0 is applied to the bottom boundary. In our study, τ_0 ranges from 10 MPa to 50 MPa, consistent with typical underfill yield strength [20]. The reference temperature is $T_0 = 25$ °C. During thermal cycling, temperature ranges from 125 °C to −40 °C. The mesh is refined until results converge. In this study, we assume temperature-independent material properties of ESL, ELK, and copper. These simplifications will affect the quantitative values but not the qualitative picture of ratcheting induced crack growth.

Fig. 3a shows the accumulated plastic deformation of the structure after 1, 100, and 1000 thermal cycles at 125 °C. For clarity, ELK is not shown. As expected, copper ratchets to the right cycle by cycle, distorting the Cu-ELK interface. Between 100 and 1000 cycles, copper no longer ratchets, and the additional deformation is small, indicating that a steady state is approached.

Fig. 3b shows the shear stress S_{12} along the bottom surface of the copper. The left end is defined as $X = 0$. After the first cycle, S_{12} is nearly uniform except near the two ends, and close to the applied shear stress $\tau_0 = 50$ MPa. After 100 cycles, S_{12} vanishes along most of the copper, except near the two ends. The copper no longer carries shear stress. The stress distribution in the copper changes negligibly between 100 and 1000 cycles, confirming a steady state. Similarly, Fig. 3c shows the shear stress S_{12} along the ESL-ELK interface, with $X = 0$ marked by the yellow circle in Fig. 3a (top). After the first cycle, S_{12} is nearly uniform and close to τ_0. After 100 cycles, S_{12} builds up in the left region of the interface,

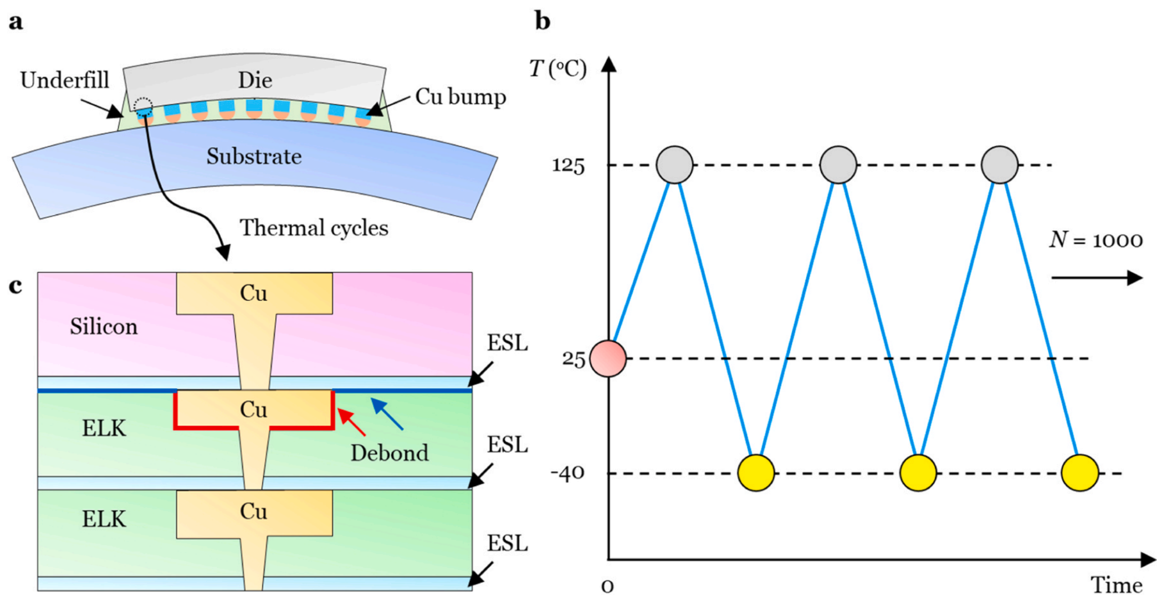

Fig. 1. Thermal cycling may cause debonding in a semiconductor device. (a) A silicon die is first bonded to a substrate via solder reflow at ∼220 °C, followed by underfill curing at $T_0 = 150$ °C. (b) The bonded structure is then cycled between −40 °C and 125 °C. (c) Illustrated at a corner of the die are several materials: silicon, etch stop layer (ESL), extreme low-κ dielectric (ELK), and copper (Cu). After thermal cycling, ESL-ELK and Cu-ELK interfaces may debond.

where stress concentration can initiate crack growth.

4. Energy release rate

Next, we introduce a crack of length $c = 50$ nm along the ESL-ELK interface (Fig. 4, inset) using the built-in seam crack function in Abaqus. The left tip of the crack is placed at the junction of the three materials. As mentioned above, the top boundary is fixed. The left and right boundaries are traction-free. A uniform shear stress is applied on the bottom boundary, pointing to the right. Given these boundary conditions, the two crack surfaces open under thermal cycling, rather than slide relative to each other. Therefore, we neglect friction between the two crack surfaces. For both ESL and ELK, the inelastic zone around the crack tip is on the order of ~1 nm, much smaller than the crack length c. Therefore, the linear elastic fracture mechanics are applicable. The energy release rate at the crack tip is computed using the built-in J-integral function in Abaqus. In this simulation, we use $w_{Cu}/t_{Cu} = 20$, $\tau_0 = 50$ MPa, and $\sigma_Y = 100$ MPa.

Initially, copper negligibly ratchets and carries most of the shear load. The crack length is small, $c = 50$ nm. The energy release rate G scales with the crack length c, and is small in the initial cycles. As temperature cycles, ratcheting in copper increases the stress in the left region of the ESL-ELK interface. In the transient regime ($N < 200$), the energy release rate G increases rapidly with the number of cycles N. After 200 cycles, copper no longer accumulates the plastic shear strain, and the energy release rate plateaus. Meanwhile, copper no longer carries shear stress and behaves like a void. Together, the void and the pre-existing crack act as an effective crack with length comparable to the width of copper, $w_{Cu} = 3$ μm. The energy release rate plateau scales with the effective crack length. Because w_{Cu} is much larger than the initial crack length c, the plateau value is much larger than the energy release rate in the initial cycles.

We next investigate the effect of the yield strength of copper, σ_Y, on the energy release rate G (Fig. 5a). In the simulation, we fix $c/t_{ESL} = 0.5$, $w_{Cu}/t_{Cu} = 20$, and $\tau_0 = 50$ MPa. The normalized yield strength σ_Y/τ_0 varies from 2 to 3.4.

For a smaller σ_Y/τ_0, copper yields over a wider temperature range during heating and cooling. Ratcheting in copper and stress buildup along the ESL-ELK interface occur more quickly. As a result, in the transient regime, G increases more rapidly with the number of cycles N. In the steady state, copper no longer ratchets and behaves like a void. Within the range of σ_Y/τ_0 explored in this study, the plateau value is nearly independent of σ_Y/τ_0.

Table 1
Geometric parameters.

Material	w (μm)	t (μm)
Copper	1.5, 3	0.15
ESL	15	0.1
ELK	15	0.25

We further study the effect of the aspect ratio of copper w_{Cu}/t_{Cu} on the energy release rate G (Fig. 5b). In the simulation, we set $c/t_{ESL} = 0.5$, $\tau_0 = 50$ MPa, and $\sigma_Y/\tau_0 = 3$. We fix $t_{Cu} = 0.15$ μm and vary w_{Cu}/t_{Cu} from 10 to 20. In both cases, during the transient regime, the energy release rate G increases rapidly with the number of cycles N. In the steady state, copper with a larger w_{Cu}/t_{Cu} behaves like a larger void. As a result, the effective crack length is larger, leading to a higher plateau value.

Notably, for copper with a larger aspect ratio, more thermal cycles are required to reach the plateau energy release rate. This trend is interpreted as follows. The thickness of copper and the overall dimension of the ESL-ELK-Cu structure are fixed. In the steady state, the applied shear stress is carried only by the ESL-ELK structure. When copper has a larger aspect ratio, the surrounding ELK is less. Consequently, the plateau shear strain is larger, and more thermal cycles are required to reach the steady state.

5. Approximation of the plateau energy release rate

We finally propose a method to approximate the plateau energy release rate using a monotonic temperature change. As discussed above, after many thermal cycles, copper no longer carries shear stress and behaves like a void. In the steady state, the effective crack length is comparable to the width of copper. This understanding allows us to further simplify the structure by replacing copper with a void (Fig. 6a). In the unsimplified structure, we use $c/t_{ESL} = 0.5$, $w_{Cu}/t_{Cu} = 20$, $\sigma_Y = 100$ MPa and simulate 1000 thermal cycles. In the simplified structure, we set $c/t_{ESL} = 0.5$, an aspect ratio of void as $w_v/t_v = 20$, and simulate a monotonic temperature increase from 25 °C to 125 °C. The shear stress τ_0 varies from 10 MPa to 50 MPa.

At different shear stress levels, the plateau energy release rate calculated from thermal cycling is well approximated by the value computed from the simplified structure under a monotonic temperature change (Fig. 6b). The slight difference is explained as follows. In the ESL-ELK-Cu structure, in the steady state, copper no longer accumulates

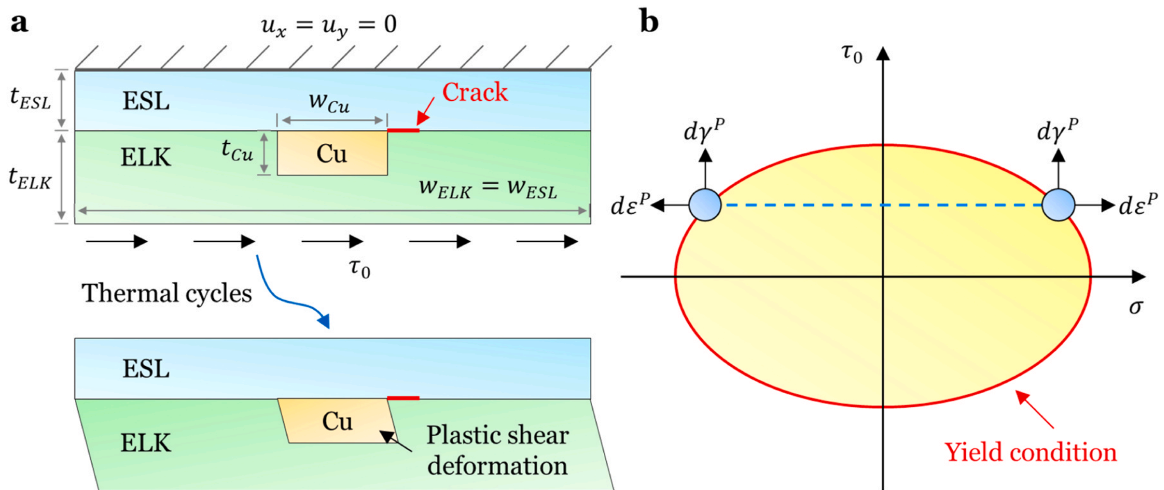

Fig. 2. The plastic ratcheting of copper caused by unidirectional shear stress and cyclic temperature. (a) Top: the undeformed structure. Bottom: the deformed structure after thermal cycles. (b) On the plane of normal stress (σ) and shear stress (τ_0), the yield condition is represented by an ellipse. During thermal cycling, the normal stress cycles, but the shear stress remains constant. The plastic shear strain accumulates cycle by cycle.

Fig. 3. Thermal cycling causes plastic deformation to accumulate and stress to redistribute. As temperature cycles, (a) plastic shear deformation accumulates, (b) the shear stress in copper vanishes, and (c) the shear stress on the ESL-ELK interface builds up. (σ_Y = 100 MPa, τ_0 = 50 MPa, and w_{Cu}/t_{Cu} = 20).

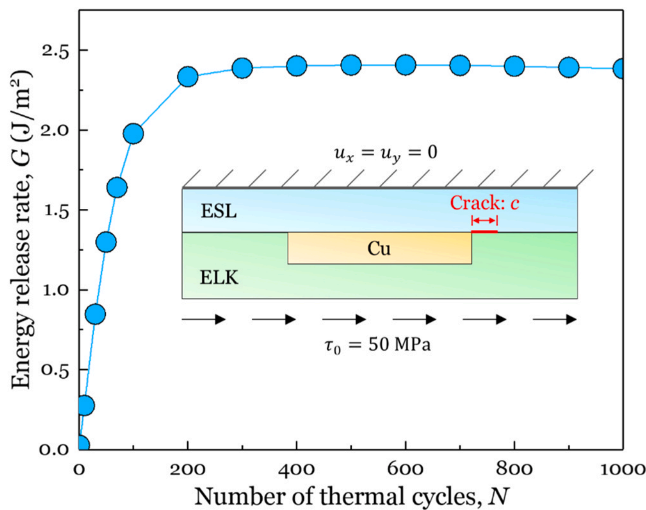

Fig. 4. As the temperature cycles, the energy release rate of a crack on the ESL-ELK interface increases.

plastic shear deformation but still undergoes cyclic normal plastic deformation. The mismatch of thermal expansion between copper and the surrounding materials induces additional stress near the crack along the ESL-ELK interface. As a result, the plateau energy release rates from the simplified and unsimplified structures differ slightly. Nevertheless, this simplification provides a good approximation of the plateau energy release rate while significantly reducing computational cost for modeling ratcheting induced cracking.

6. Conclusions

We have studied crack growth in brittle materials caused by ratcheting plastic deformation in a nearby metal. When temperature cycles, the plastic deformation in the metal ratchets, and the energy release rate of a crack in nearby brittle materials increases. After many thermal cycles, the metal no longer ratchets and carries negligible shear stress, and the energy release rate plateaus. We find that this plateau can be well approximated using a simplified structure in which the metal is replaced by a void, calculated using a monotonic temperature change. We also examine how the energy release rate depends on material and geometric parameters. In the transient regime, a lower metal yield strength leads to faster buildup of the energy release rate. However, the plateau energy

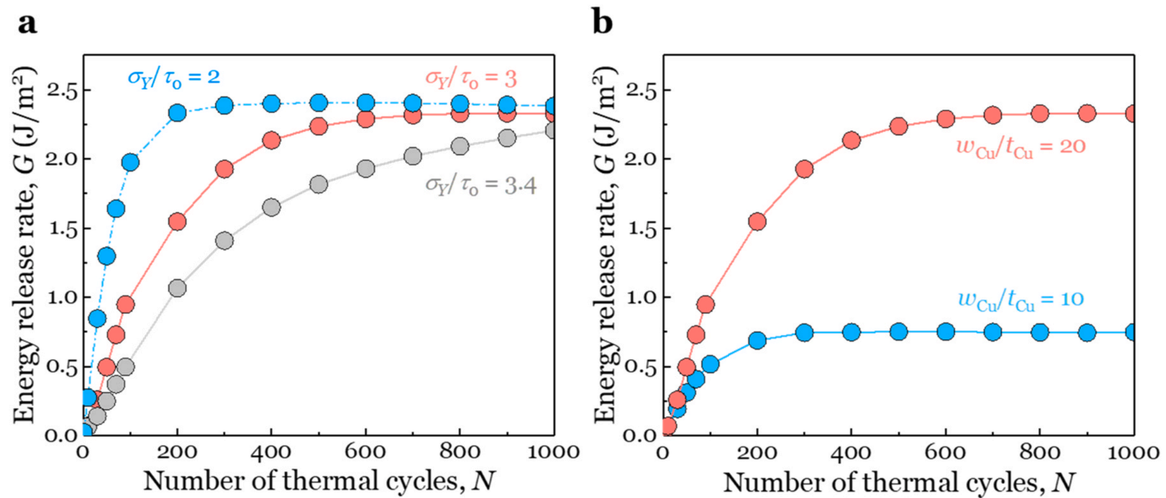

Fig. 5. The effect of (a) yield strength σ_Y and (b) aspect ratio of copper w_{Cu}/t_{Cu} on the energy release rate G over thermal cycles.

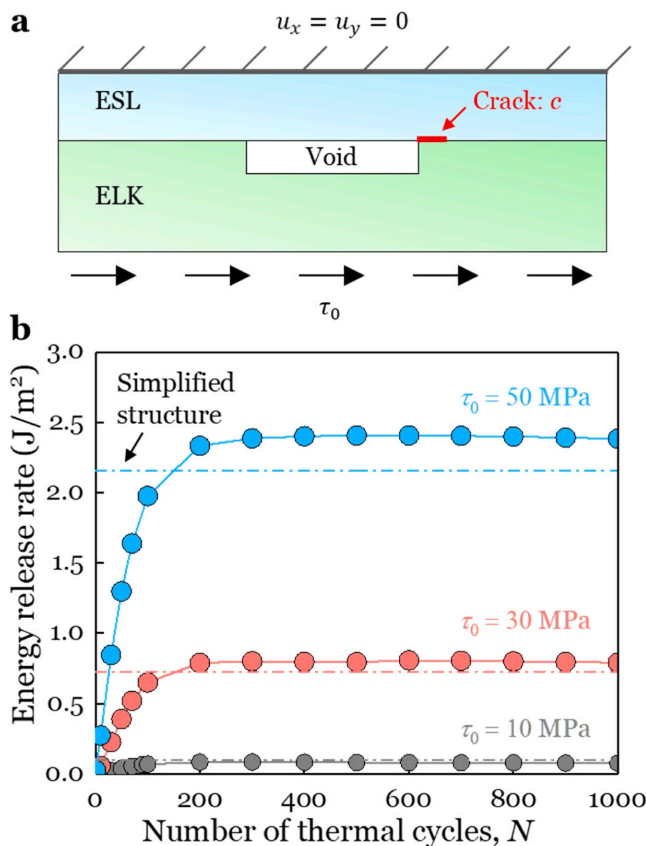

Fig. 6. Approximation of the plateau energy release rate. (a) Simplified structure with copper replaced by a void. (b) Plateau energy release rate from the simplified structure, compared with the energy release rate from the unsimplified structure under thermal cycling.

release rate is nearly independent of yield strength. Furthermore, a larger aspect ratio of the metal leads to a larger effective crack length and thus a higher plateau energy release rate. This study provides an understanding of ratcheting-induced crack growth in semiconductor devices under thermal cycling. We hope that this work will aid in the design of semiconductor devices.

CRediT authorship contribution statement

Chenghai Li: Writing – review & editing, Writing – original draft, Methodology, Investigation, Formal analysis, Conceptualization. **Shao-Chen Tseng:** Writing – review & editing, Methodology, Investigation, Formal analysis. **Yu Zhou:** Writing – review & editing, Methodology, Investigation, Formal analysis. **Chieh-Hao Hsu:** Investigation. **Wei-Hsiang Tu:** Investigation. **Kuo-Chin Chang:** Investigation. **Jun He:** Funding acquisition. **Zhigang Suo:** Writing – review & editing, Writing – original draft, Supervision, Methodology, Funding acquisition, Conceptualization.

Declaration of Competing Interest

The authors declare that they have no known competing financial interests or personal relationships that could have appeared to influence the work reported in this paper.

Acknowledgment

The work at Harvard was supported by a contract from TSMC.

Data availability

Data will be made available on request.

References

[1] J.H. Lau, Recent advances and trends in advanced packaging, IEEE Trans. Compon. Packag. Manuf. Technol. 12 (2) (2022) 228–252.
[2] D. Shamiryan, T. Abell, F. Iacopi, K. Maex, Low-*k* dielectric materials, Mater. Today 7 (1) (2004) 34–39.
[3] P.G. Neudeck, Progress in silicon carbide semiconductor electronics technology, J. Electron. Mater. 24 (1995) 283–288.
[4] Z. Zhang, C.P. Wong, Recent advances in flip-chip underfill: materials, process, and reliability, IEEE Trans. Adv. Packag. 27 (3) (2004) 515–524.
[5] B. Wang, J. Cai, X. Du, L. Zhou, Review of power semiconductor device reliability for power converters, CPSS Trans. Power Electron. Appl. 2 (2) (2017) 101–117.
[6] G.B. Alers, K. Jow, R. Shaviv, G. Kooi, G.W. Ray, Interlevel dielectric failures in copper/low-*k* structures, IEEE Trans. Device Mater. Reliab. 4 (2) (2004) 148–152.
[7] K. Lim, The many faces of absorptive capacity: spillovers of copper interconnect technology for semiconductor chips, Ind. Corp. Change 18 (6) (2009) 1249–1284.
[8] Y.-L. Shen, Analysis of thermal stresses in copper interconnect/low-*k* dielectric structures, J. Electron. Mater. 34 (2005) 497–505.
[9] A.A. Volinsky, J.B. Vella, W.W. Gerberich, Fracture toughness, adhesion and mechanical properties of low-K dielectric thin films measured by nanoindentation, Thin Solid Films 429 (1-2) (2003) 201–210.
[10] M. Huang, Z. Suo, Q. Ma, Metal film crawling in interconnect structures caused by cyclic temperatures, Acta Mater. 49 (15) (2001) 3039–3049.

[11] M. Huang, Z. Suo, Q. Ma, Plastic ratcheting induced cracks in thin film structures, J. Mech. Phys. Solids 50 (5) (2002) 1079–1098.
[12] M. Huang, Z. Suo, Q. Ma, H. Fujimoto, Thin film cracking and ratcheting caused by temperature cycling, J. Mater. Res. 15 (6) (2000) 1239–1242.
[13] M.R. Begley, A.G. Evans, Progressive cracking of a multilayer system upon thermal cycling, J. Appl. Mech. 68 (4) (2001) 513–520.
[14] S.H. Im, R. Huang, Ratcheting-induced wrinkling of an elastic film on a metal layer under cyclic temperatures, Acta Mater. 52 (12) (2004) 3707–3719.
[15] M.A. El Khakani, M. Chaker, A. Jean, S. Boily, J.C. Kieffer, M.E. O'hern, M.F. Ravet, F. Rousseaux, Hardness and young's modulus of amorphous a-SiC thin films determined by nanoindentation and bulge tests, J. Mater. Res. 9 (1) (1994) 96–103.
[16] K.M. Jackson, Fracture strength, elastic modulus and poisson's ratio of polycrystalline 3C thin-film silicon carbide found by microsample tensile testing, Sens. Actuators A Phys. 125 (1) (2005) 34–40.
[17] D.N. Talwar, J.C. Sherbondy, Thermal expansion coefficient of 3C-SiC, Appl. Phys. Lett. 67 (22) (1995) 3301–3303.
[18] X.H. Liu, M.W. Lane, T.M. Shaw, E.G. Liniger, R.R. Rosenberg, D.C. Edelstein, Low-k BEOL mechanical modeling, Proc. Adv. Met. Conf. (2004) 361–367.
[19] X. Gao, R. Chen, T. Liu, H. Fang, G. Qin, Y. Su, J. Guo, High-entropy alloys: a review of mechanical properties and deformation mechanisms at cryogenic temperatures, J. Mater. Sci. 57 (12) (2022) 6573–6606.
[20] Z. Qian, J. Wang, J. Yang, S. Liu, Visco-elastic-plastic properties and constitutive modeling of underfills, IEEE Trans. Compon. Packag. Technol. 22 (2) (1999) 152–157.